

Finite Element Modelling of Log Wall Corner Joints

R. Kalantari, G. Hafeez

Abstract—The paper presents outcomes of the numerical research performed on standard and dovetail corner joints under lateral loads. An overview of the past research on log shear walls is also presented. To the authors' best knowledge, currently, there are no specific design guidelines available in the code for the design of log shear walls, implying the need to investigate the performance of log shear walls. This research explores the performance of the log shear wall corner joint system of standard joint and dovetail types using numerical methods based on research available in the literature. A parametric study is performed to study the effect of gap size provided between two orthogonal logs and the presence of wood and steel dowels provided as joinery between log courses on the performance of such a structural system. The research outcomes are the force-displacement curves. Variability of 8% is seen in the reaction forces with the change of gap size for the case of the standard joint, while a variation of 10% is observed in the reaction forces for the dovetail joint system.

Keywords—Dovetail joint, finite element modelling, log shear walls, standard joint.

I. INTRODUCTION

LOG houses have been the typical construction style of the countryside, introduced to Canada by new settlers of Europe. This pre-historic construction technology is emerging again in North America, even in seismic-prone regions, with new modifications to accommodate today's lifestyle. Currently, there are more than 400,000 log homes in North America [1], [2] serving as temporary cabins and trappers to the homes and cottages. Model building code does not provide comprehensive information required for designing log shear walls.

The construction industry adopts diverse methods for building log houses, including milled and handcrafted, which differs significantly in their construction order. A milled, often known as a factory-made log, has been put through a sawmill and cut into a uniform shape and size, while handcrafted logs are hand peeled. In factory-made log houses, floor systems offer various choices ranging from conventional wood joists to engineered floor trusses. Subflooring consists of plywood sheets attached to the joist system using screws, nails and/or adhesives. Once the walls are erected, the second-floor system is installed. In the handcrafted method, the bark is removed from round logs with a traditional woodworking hand tool first, while the square-style logs are shaped at the lumber mill. Finally, the handcrafted appearance of the log is produced using different hand tools. A handcrafted log home provides an appealing aesthetic with a variety of log profiles and corner systems. Fig. 1 and Fig. 2 show commonly used log profiles and wall corner systems. Each corner system provides different behavior under different load patterns, and their selection is

entirely dependent on project expectation. These joints need sophisticated carpentry to create tightness among log layers.

The subsequent section summarizes the past studies on log-house walls followed by a parametric study performed in the current study.

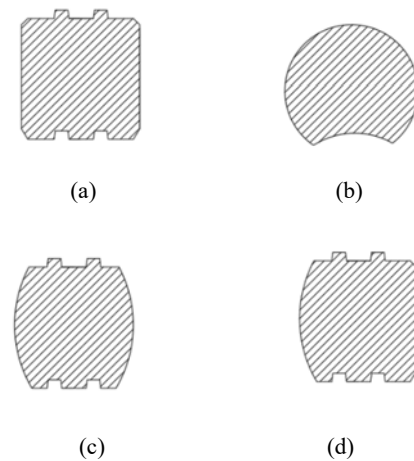


Fig. 1 Common profile sections in log-walls a) Square log b) Swedish cope log c) Round log d) D profile log

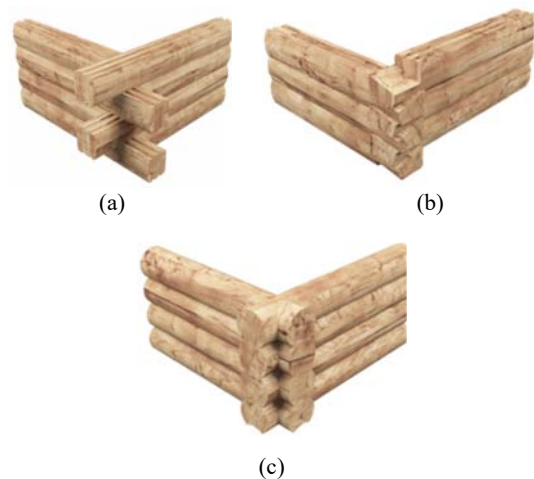


Fig. 2 Common corner joint used in log-walls a) butt and pass corner style b) dovetail joint c) interlocking corner

II. PAST STUDIES

A. Friction Model by Hahney (2000)

Hahney described the behavior of log walls under lateral forces (seismic and wind) based on log joinery, log-to-log friction and interlocking hardware. The author emphasized the

G. Hafeez is with the Concordia University, Canada (corresponding author, phone: e-mail: ghazanfarah.hafeez@concordia.ca).

R. Kalantari was with the Concordia University, Canada (e-mail: reza.kalantari@mail.concordia.ca).

corner interlocking by notches and the long grooves providing resistance to lateral loads given the uplift is under control. It was indicated that the logs of sidewalls could be stabilized by the load transfer through long grooves of the windward wall to the lower log layer and so on [3].

B. Experimental and Numerical Studies

The author performed friction, static and quasi-static tests on sill log-foundation anchorage of two commonly available construction systems, i) sill log mounted on the floor diaphragm and ii) sill log in direct contact with the sill plate. The findings suggested that the sill logs dissipate energy, and the resistance provided by the connections against lateral loads is more than the required [4].

Monotonic and reverse-cyclic tests were conducted on log shear walls, and their performance was compared to light-frame wood, concrete, and masonry shear walls. Each wall was built using ten full courses and one sill log (the last log sitting on the foundation) with three different dimensions and aspect ratios of 1:1 (height- 2.4 m, length- 2.4 m), 2:1 (height- 1.2 m, length- 2.4 m), and 4:1 (height- 2.4 m, length- 0.6 m). The findings indicated higher resistance provided by log shear walls than of light-frame wood shear walls. Further, the results of the wall with 1:1 aspect ratio showed higher horizontal shear strength values than light-frame walls, as indicated in the literature by [5], [6].

An overview of log house's performance under seismic events was evaluated after a complex type earthquake hit the Kaikoura area in 2016. The majority of the houses were built using machined logs available locally on a concrete slab attached to the foundations. However, few were witnessed built with hand-hewed logs and with other construction details. Fig. 3 shows one of the typical houses in that area. In general, the log houses performed well, with the exception of few houses that cannot be repaired. The horizontal sliding between the logs was found to be the main reason for the majority of the house's damage, leading to impairment of non-structural components, while the minimum damages were seen to the foundations. Further, damage to vertical tie-down rods was observed frequently, either due to tensile loads or the loosening caused by shrinkage in the logs [7].



Fig. 3 Constructed log-house in Kaikoura area [7]

Cyclic and monotonic tests were performed on Blockhaus shear walls with similar geometry but different corner joints provided at the end of the shear wall. Quasi-static tests were also performed to assess their in-plane shear capacity and

flexibility. The test procedure ensured the practice was adopted for Blockhaus systems. A numerical model was developed and calibrated with the test results. The authors concluded elevated shear resistance of the tested walls when subjected to in-plane seismic loads. Also, high deformation limit was obtained when comparing to ultimate lateral displacement of light-frame wood shear walls or masonry-filled timber-framed walls under in-plane lateral loads [8].

In another study, monotonic and cyclic tests were performed to investigate the in-plane behavior of two different log house construction systems; i) the Standard half-lapped joint (ST) system and ii) Tirolerschloss joint (TR) systems were investigated. The experimental program was consisting of corner joint testing and full-scale shear wall tests. The corner joint tests were conducted for developing load-displacement curves and for assessing the strength and stiffness characteristics of different corner geometries. The full-scale shear wall consists of seventeen logs, with the two last rows of logs fastened together with screws, and the loading was applied in both horizontal and vertical loading. The outcome of the research suggested friction between the logs, construction tolerances/gaps and the behavior of corner joints as prevailing parameters on lateral behavior of the tested walls. A higher capacity of the wall was observed with ST corner joint. Further, the rheological model developed in this study was found sufficient for predicting the log wall behavior [9].

III. STRUCTURAL DESIGN AND RESPONSE OF LOG WALLS

Log shear walls are bearing walls that resist lateral loads and gravity loads. Generally, friction between log layers and the corner notches provide resistance against internal shear force and self-weight of the wall along with vertical steel rods resisting the overturning [7]. The shear force at the base of the walls is transferred through the bottom-most log of the wall to the foundation by anchorages.

The gravity design of log houses is relatively simple but requires an appropriate plan for controlling shrinkage in log walls. The load from upper levels is supported by the log walls positioned at internal and external locations. These walls are primarily exposed to low compression perpendicular to the grain due to the large cross-section of the supporting structures.



Fig. 4 Prince Edward County, 1790 [10]

However, the lateral deformation of log shear walls is not straightforward to be assessed as such general design rules for wooden shear walls are not applicable to log walls due to their low lateral resistance comparative to other wooden shear walls. Simultaneously, their satisfactory performance over the years

demonstrated their potential candidacy to withstand lateral loads. Fig. 4 and Fig. 5 show photos of log houses built in the 17th and 18th centuries.



Fig. 5 Simco county, 1850 [10]

IV. FINITE ELEMENT (FE) MODEL CHARACTERIZATION

A finite element method is a reliable approach for predicting structural behavior under various loading scenarios. The work presented here is a step towards a comprehensive numerical investigation of log-house shear walls with standard and dovetail corner joints under lateral loads. A finite element model is developed in ABAQUS [11] using 3D solid elements 8-node, C3D8R type, was verified with the literature [12]. The dimensions and material properties of the specimen were chosen based on previous studies, aiming to calibrate the model with available experimental results [8], [12], [13]. A typical log wall joint specimen profile consists of five timber logs, three corresponding to in-plane lateral directions and the rest in the orthogonal direction. Fig. 6 and Fig. 7 show the dimension details of standard and dovetail joint specimens.

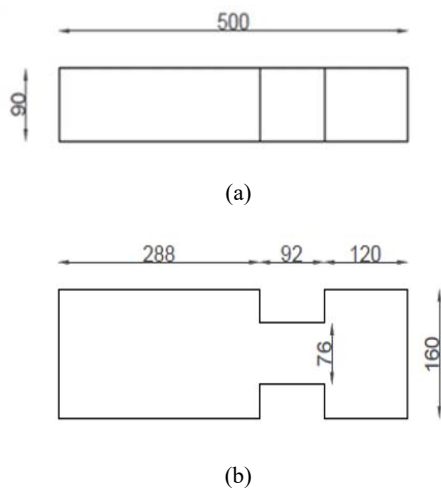


Fig. 6 FE-model dimension of standard joint a) top view b) side view

The FE model was validated with the past studies available in the literature [9], [12], [13]. Comparative behavior of the force-displacement curves obtained from the current study and the test data (FE-STRU) available in the literature [12] is shown in Fig. 8.

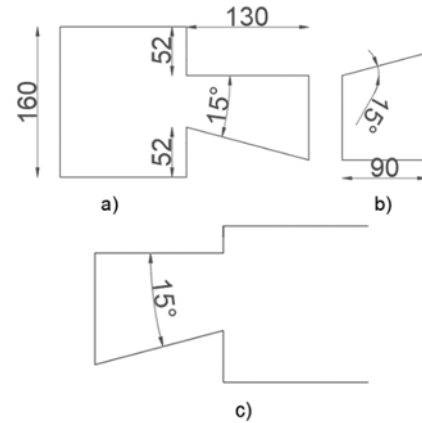


Fig. 7 Dovetail dimensions detail a) front view b) end view c) front view

A reasonable agreement is seen between the results with the deviation of 2-3% that could correspond to the difference in modeling technique as such the number of incremental approaches chosen in ABAQUS [11] in step module and the number of seeds for generating mesh size.

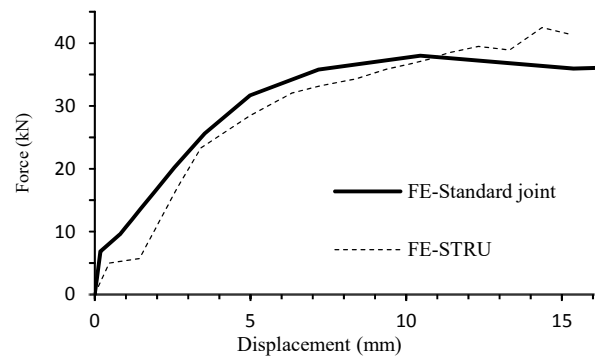


Fig. 8 Force-displacement curve comparison between FE-standard joint model (current study) and FE-STRU from the literature [12]

Once the geometry is completed, the interface connection between the surfaces of timber logs was assigned as the penalty approach, with a static friction coefficient of 0.5 for timber-to-timber contact, and the normal behavior was defined as hard contact. The analysis followed two steps; i) the specimens are compressed together with an initial compressive load from top to bottom, followed by ii) the displacement imposed on the top log in the main log direction, obtaining a reaction force and the corresponding deflection relationship. The main log movement is restricted by defining boundary conditions allowing movement only in the main log direction. However, the bottom log in the main direction is restricted ($X=Y=Z=0$). Fig. 9 provides a visualization of the loading procedure. The vertical loads compress the specimen keeping log layers intact in a sequence while imposing lateral displacements to the top most log layer in the main direction.

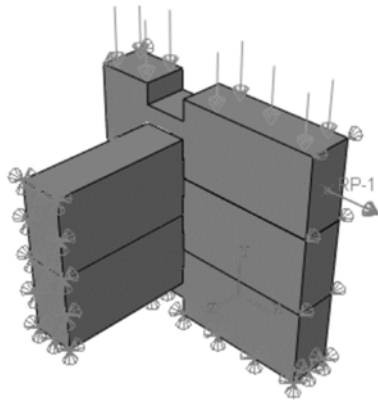


Fig. 9 Boundary condition and loading scenario

The deformed and unreformed geometries of the standard joint model are shown in Fig. 10.

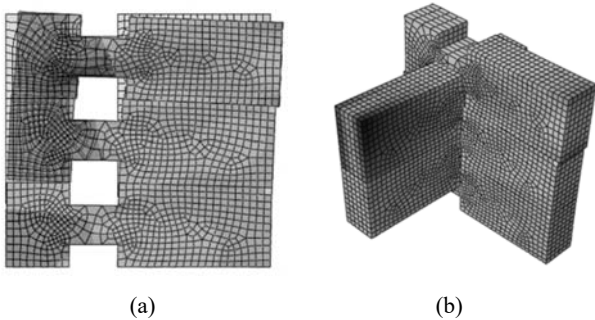


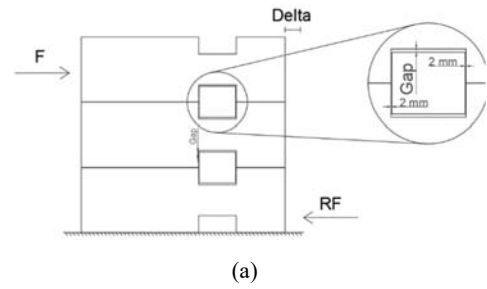
Fig. 10 FE models showing a) deformed and un-deformed geometries
 b) S misses max distribution in the main log (6 mm gap)

A. Parametric Study

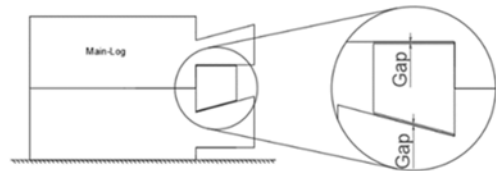
A parametric study was performed on log wall corner specimens of standard and dovetail joints to assess the effect of gap size between two orthogonal logs (provided for construction details such as insulation/engineering tolerances) on the reaction force [8], [12], [13]. The study further explores the effect of wood and steel dowels joining two log layers on the reaction force.

Multiple FE models were developed for standard and dovetail corner joints with variable gap sizes (2 mm to 6 mm - standard joint) and (0 mm to 2 mm - dovetail). A schematic of standard and dovetail joints demonstrating gap orientation can be seen in Fig. 11. Results corresponding to each joint type are displayed in TABLE I.

First, the FE models were modified considering wood dowel (diameter of 10 mm), which then altered further, replacing a steel dowel instead. Standard joint FE models, FE-SG6 and FE-SG4 were modified to FE-SG6-Dowel and FE-SG4-Dowel, respectively, for studying the effect of wood dowel on maximum reaction force. FE-SG6 and FE-SG4 were then developed by replacing the wood dowels with steel, and the material properties were provided according to the literature [14].



(a)



(b)

Fig. 11 Vertical gap description in the main-log direction in a) standard joint FE-model and b) dovetail FE-model

The comparative results between the models with dowels of different materials are provided in TABLE II. Fig. 12 shows a schematic of standard joint specimen detail, including dowel, while Fig. 13 displays dowel rupture under imposed displacement.

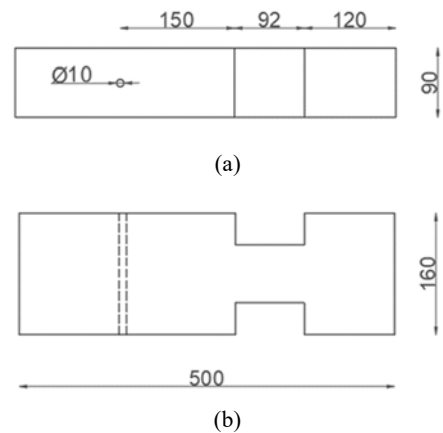


Fig. 12 Specimen detail for dowel location a) top view and b) side view

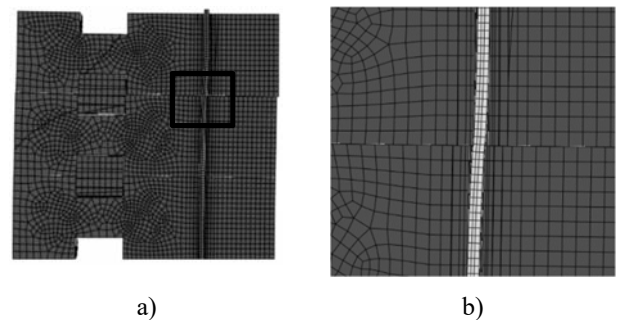


Fig. 13 FE model showing a) deformed dowel part b) the rupture of dowel under imposed displacement

B. Results

In general, the FE model provides reliable results for the corner joints; 8% variability is seen in the reaction forces with the change of gap size for the case of standard joint, with reaction force value ranging from 38.02 kN to 41.39 kN. While in dovetail joints, the variation of approximately 10% is observed in the reaction forces by altering the gap dimensions, with an inverse relationship between gap size and the reaction force. Generally, dovetail shape needs more sophisticated industrial machines to produce accurate shapes for enhanced structural performance.

TABLE I
 RESULTS OF STANDARD AND DOVETAIL CORNERS JOINT SPECIMENS WITH GAP VARIATION

FE models	Joint types	Gap	Max R-force (kN)	Displacement (mm)
FE-SG2	Standard Joint	2	39.30	11.43
FE-SG4	Standard Joint	4	38.02	10.45
FE-SG6	Standard Joint	6	41.39	11.43
FE-DG0	Dovetail joint	0	52.08	4.72
FE-DG0.5	Dovetail joint	0.5	51.29	4.80
FE-DG1	Dovetail joint	1	49.24	4.82
FE-DG2	Dovetail joint	2	45.40	4.87

Fig. 14 and Fig. 15 show the relation between maximum reaction forces and the corresponding displacements for standard and dovetail joints. Initially, the stiffness for different FE models shown in Fig. 14 is quite alike; however, FE-SG4 showed earlier deformation than the other two models. The reason could be the dimension of the gap all around the corner, as the gap provided in each direction (orthogonal and main log) is 4 mm, allowing convenient slippage than the models with other dimensions leading to the minimum reaction force at the bottom log (see Fig. 14).

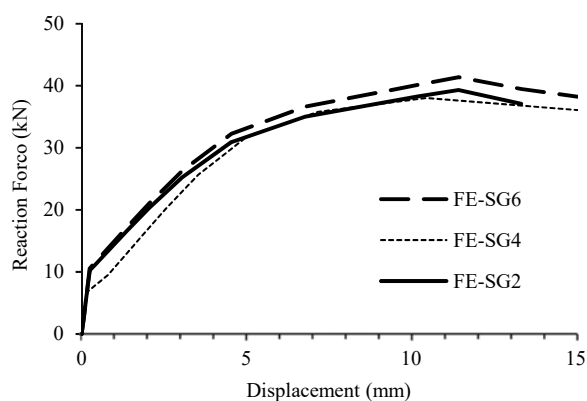


Fig. 14 Reaction force-displacement curve for standard joint (FE-SG6, FE-SG4, FE-SG2)

No significant difference is noticed for initial stiffness in the case of the dovetail joint (see Fig. 15). Unlike force-displacement behavior observed for the case of standard joint (see Fig. 14), slippage is not seen for the case dovetail joint (see Fig. 15). In standard joint FE models, the gap is provided in two

orthogonal directions. However, no gap is provided in the main log direction for the dovetail joint (see Fig. 11), preventing slippage in the force-deflection curve. Further, an inverse relationship between the size of the gap and the reaction force is observed from Fig. 15, where maximum reaction force is seen for FE-DG0.5 and minimum reaction force for model FE-DG2.

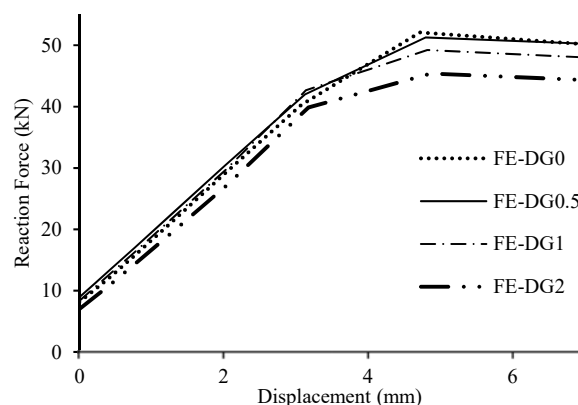


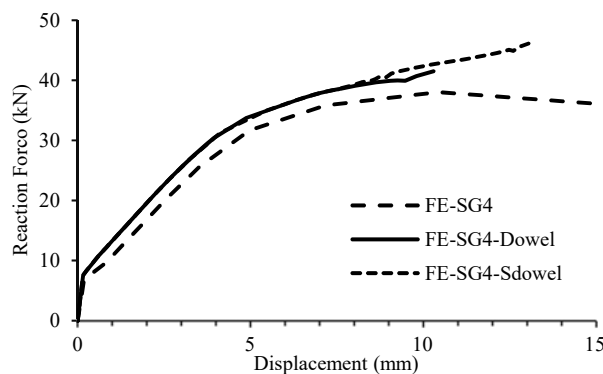
Fig. 15 Reaction force-displacement curve for dovetail joint (FE-DG0, FE-DG0.5, FE-DG1, FE-DG2)

The results from TABLE II indicate an improved response of log corners with standard and dovetail type joints by introducing wood and steel dowels. A 5% to 10% increase is seen when the wood dowel is added to the model, which further increased to 15% when the wood dowel was replaced with the steel one.

TABLE II
 RESULTS OF FE MODELS WITHOUT DOWEL AND WITH DOWEL

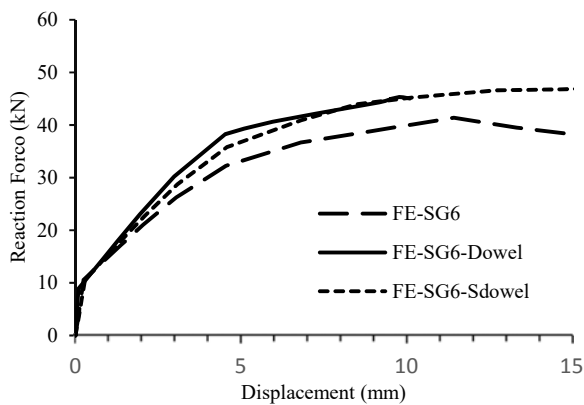
Items	Without dowels		Wood dowel		Steel dowel	
	FE-SG6	FE-SG4	FE-SG6-Dowel	FE-SG4-Dowel	FE-SG6-SDowel	FE-SG4-SDowel
Reaction force (kN)	41.3	38.0	45.3	39.9	47.1	44.8
Displacement (mm)	11.4	9.7	9.7	9.2	16.5	12.6

A force-displacement comparison is shown in (a)

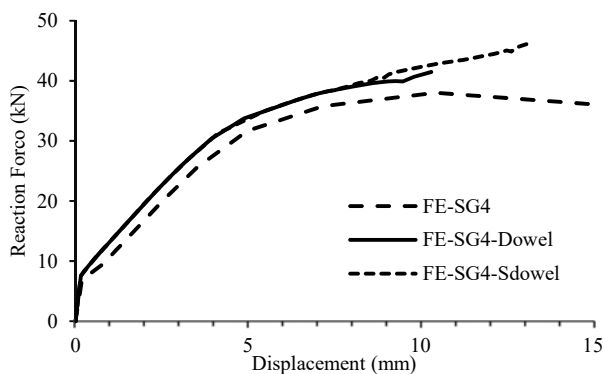


(b)

Fig. 16 (a) and Fig. 16(b) for both steel dowel (FE-SG6-Sdowel) and wood dowel (FE-SG6-Dowel) specimens when comparing with the reference FE model (FE-SG6) for standard joint corner system. It can be noticed that ultimate resistance (reaction force) is increased by introducing either steel or wood dowel to FE-SG6. However, the gap provided between the logs oriented in two orthogonal directions offers sliding between two orthogonal logs. Similar findings are found in the literature but for different joint detail [14]. Further, a smooth curve is seen for the case of steel dowel followed by extended displacement versus increased reaction force, while the curve of wood dowel shows crushing.



(a)



(b)

Fig. 16 Reaction force-displacement curve comparison of a) FE-SG6, FE-SG6-Dowel and FE-SG6-Sdowel b) FE-DG0, FE-DG0-Dowel and FE-DG0-Sdowel

ACKNOWLEDGMENT

The authors greatly acknowledge the financial support provided by Concordia University Seed Funds.

REFERENCES

[1] P. Marjan, B. Deacon and E. Karacabeyli, "Testing of lateral resistance of handcrafted log walls Phase I and II," *International Log Builders Association*, 2002.
 [2] National Association of Home Builders NAHB," NAHB Web Site, Jan 2007. (Online).
 [3] T. Hahney, "How log buildings resist lateral loads," *Log Building News; Number 32*, 2000.

[4] R. J. Scott, R. J. Leichti and T. H. Miller, "An experimental investigation of foundation anchorage details and base shear capacity for log buildings," *Forest Products Journal*, vol. 55, no. 4, pp. 38-45, 2005.
 [5] A. Salenikovich, "The racking performance of light-frame shearwalls," *Ph.D. dissertation, Virginia Tech*, 2000.
 [6] D. A. Graham, D. M. Carradine, D. A. Bender and J. D. Dolan, "Performance of log shear walls subjected to monotonic and reverse-cyclic loading," *Journal of Structural Engineering*, vol. 136, no. 1, pp. 37-45, 2010.
 [7] A. Buchanan and D. Moroder, "Log house performance in the 2016 Kaikoura earthquake," *Bulletin of the New Zealand Society for Earthquake Engineering*, vol. 50, no. 2, pp. 225-236, 2017.
 [8] C. Bedon, M. Fragiocomo, C. Amadio and C. Sadoc, "Experimental study and numerical investigation of blockhaus shear walls subjected to in-plane seismic loads," *Journal of Structural Engineering*, vol. 141, no. 4, 2015.
 [9] P. Grossi, T. Sartori, I. Giongo and R. Tomasi, "Analysis of timber log-house construction system via experimental testing and analytical modelling," *Construction and Building Materials*, vol. 102, pp. 1127-1144, 2016.
 [10] B. Coffey, "From shanty to house: log construction in nineteenth-century Ontario," *International Society for Landscape, Place & Material Culture*, vol. 16, no. 2, pp. 61-75, 1984.
 [11] Abaqus, F.E.A. V. 6.12 Computer Software; Dassault Systèmes: Providence, RI, USA, 2015.
 [12] M. Sciomenta, C. Bedon, M. Fragiocomo and A. Luongo, "Shear performance assessment of timber log-house walls under in-plane lateral loads via numerical and analytical modelling," *Buildings*, vol. 8, no. 8, pp. 99, 2018.
 [13] T. Giovannini, P. Grossi and R. Tomasi, "Blockhaus system: Experimental characterization of corner joints and shear walls," *In Proceedings of the World Conference on Timber Engineering*, pp. 10-14, 2014.
 [14] C. Bedon and M. Fragiocomo, "Numerical investigation of timber log-haus walls with steel dovetail reinforcements under in-plane seismic loads," *Advances in Civil Engineering*, 2018.